Optothermal Properties of Fibers. VI. Effect of Annealing on Some of the Optical and Dynamic Mechanical Parameters of Polyester Fibers

A. A. HAMZA, I. M. FOUDA,* M. M. EL-TONSY, and F. M. EL-SHARKAWY

Physics Department, Faculty of Science, Mansoura University, Mansoura, Egypt

SYNOPSIS

Changes in the structure of annealed polyester fibers (Egyptian manufacture) at a constant time of 5 h and different temperatures (80–190°C) were studied interferometrically. The Pulta polarizing interference microscope was used for determining the mean refractive indices and mean birefringence of these fibers. The multiple-beam Fizeau fringes in transmission was also used for determining the refractive indices of the skin and core of these fibers. Also, the acoustic method was used for measuring the density and mechanical loss factor of these fibers. Relations between the mean refractive indices, birefringences polarizabilities per unit volume, and mechanical parameters of annealed polyester fibers with different temperatures are discussed to clarify the thermal effects. Illustrations are given using graphs and microinterferograms.

INTRODUCTION

An isotropic polymer has the same structure and properties in all directions. Upon deformation in the solid state, the polymer becomes anisotropic because the polymer chains align and therefore become oriented with respect to a particular direction. The degree of orientation with respect to a particular direction expresses a measure of the extent of anisotropy produced by the deformation process. Since the properties of an anisotropic polymer show a directional dependence, a measurement of the orientation in the polymer portrays how its properties are modified during deformation.

To measure the orientation in a polymer, there are a number of different techniques, depending on its constitution.[1] The use of interferometric methods is of considerable importance to provide information about the degree of orientation in a molecular system. Applications of double-beam or multiple-beam interferometry were used to evaluate the effect of mechanical, thermal, or chemical treatments of natural and man-made fibers.[2–8]

Part of the modern trend in fiber research is to alter fiber properties; one of the methods for property modification involves the effect of the annealing process at different conditions. Several studies have been reported on the effect of annealing on the structure of synthetic and natural fibers.[9–13]

One of the principal methods of investigation of molecular motion in polymers is to study the temperature dependence of the parameters characterizing the dynamic mechanical properties, especially the temperature dependencies of mechanical losses. The change of the intermolecular interaction energy due to thermal treatment has an effect not only on molecular motion in the polymer but also on the value and nature of mechanical losses.[14]

In the present work, the effect of annealing was studied for the density mechanical loss factor and optical properties of polyester (PET, Egyptian manufactures). Two-beam, multiple-beam, and resonance techniques were used to study the temperature dependence of the parameters char-

For Part I of this study, cf. Ref. 17. Parts II–V will appear in a future issue of this journal.

* To whom correspondence should be addressed.

Journal of Applied Polymer Science, Vol. 59, 1585–1596 (1996)
 CCC 0021-8995/96/101585-12

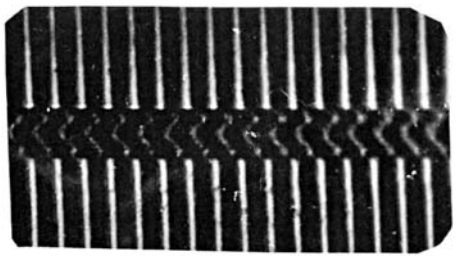

Plate (1-a)

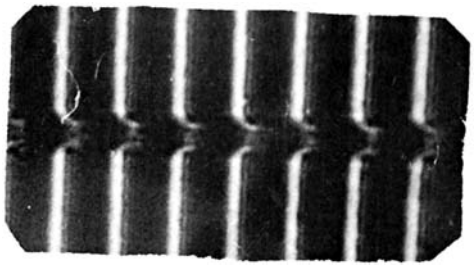

Plate (1-b)

Plate 1 (a,b) Microinterferograms of multiple-beam Fizeau fringes in transmission for the parallel and perpendicular directions of untreated PET fiber.

acterizing the optical and dynamic mechanical properties.

EXPERIMENTAL

Sample Preparation: Annealing

Polyester fibers were distributed in a cocoon form on glass rods with free ends which were then heated in an electric oven whose temperature was variable from 80–190°C ± 1°C at a constant time of 5 h, then left to cool at room temperature, 28 ± 1°C.

Measurement of Cross-Sectional Area

The method discussed in detail in Ref. 15 for measuring the fiber diameter was used. Twenty fibers were chosen at random from the Egyptian polyester fibers to be tested. Light from a He—Ne laser source (λ = 632.8 nm) was incident normally to the fiber axis. The diffraction pattern was observed on the screen. The fiber was scanned at nine orientations separated by an angle of 40° about its axis. Figure 1 gives some experimental results for the cross-sectional view of the polyester fibers. According to these figures, the cross-sectional view shows a perfectly circular shape.

Determination of Density and Mechanical Loss Factor of (PET) Polyester Fibers Using the System of Vibration

For the measurement of fiber density, a special measuring system previously constructed and explained in detail was used.[16,17] The apparatus for this system was based on the concept of vibrating strings. It is well known that when a string is stretched by a tensional force, T, and put in contact with a vibrator which vibrates at right angles to the axis of the string, a definite length, L, of the string will vibrate stationary as the resonance condition between frequencies of the vibrator and string is achieved. Let f_0 be the resonance frequency; then

$$f_0 = (P/2L)(T/m)^{1/2} \quad (1)$$

where P is the number of resonance modes within the string length, $L(P = 1$ for the fundamental mode) and m is the mass per unit length of the string.[18] Using such a system allows determination of the fundamental resonance frequency, f_0, of a certain length, L, of the sample (L is the distance between the vibrator and receiver) when it is loaded by a mass, $M(g)$. Then, the mass per unit length, m, of the sample under the test could be calculated from eq. (1). An accurate value of m could be obtained as an average over several modes of resonance.

From the obtained value of m, the density, ρ, of the sample material can be easily calculated to an accurate 3×10^{-3}. If the sample is taken as bundle of N individual fibers per bundle,

$$\rho = gM/4\Pi NL^2r^2f_0^2 \quad (2)$$

where g is the acceleration due to gravity, and r, the radius of an individual fiber.

The mechanical loss factor, tan δ, of the annealed fibers was measured by the same system which is

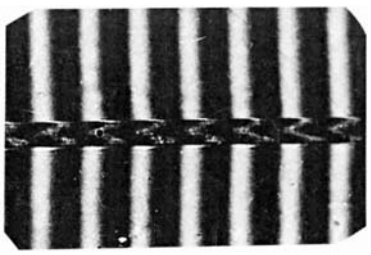

Plate (2-a)

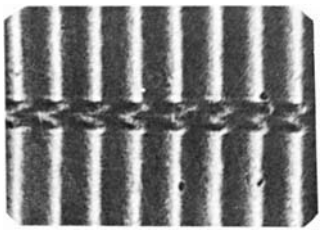

Plate (2-c)

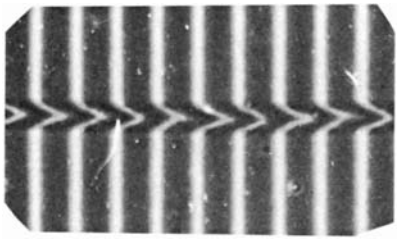

Plate (2-b)

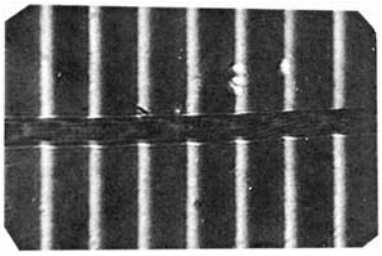

Plate (2-d)

Plate 2 (a–d) Microinterferograms of multiple-beam Fizeau fringes in transmission for the parallel directions of PET fiber with annealing temperature 80, 100, 120, 140°C, respectively, at a constant time of 5 h.

used for the density determination. The mechanical loss factor, tan δ, can be determined using the following formula[19,20]:

$$\tan \delta = \Delta f / f_0 \tag{3}$$

where f_0 is the high frequency and $\Delta f = f_2 - f_1$ is the half-bandwidth of the resonance curve. The following measuring conditions had been satisfied for high accuracy:

(a) The fiber diameter is sufficiently narrow in such a way that the shift in the resonance frequency due to air damping could neglected.
(b) The length of the fiber should be selected in such a way that the resonance frequency is located within a frequency region completely free from any other resonance peaks due to natural frequencies of the system. This avoids the effect of resonance coupling.
(c) The loading mass should be sufficiently small to avoid any serious structural variations due to the mechanical creep in the same sample.

Multiple-Beam Fizeau Fringes Technique

Multiple-beam interferometric methods were applied to determine the mean refractive index and birefringence of polyester fibers. The interference fringes produced from the multiple-beam interfer-

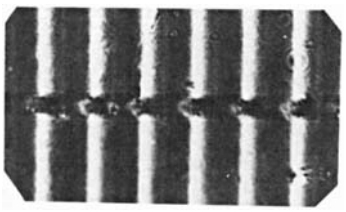

Plate (3-a)

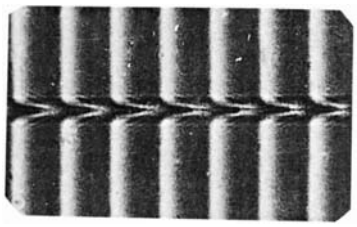

Plate (3-e)

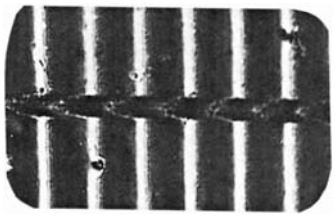

Plate (3-b)

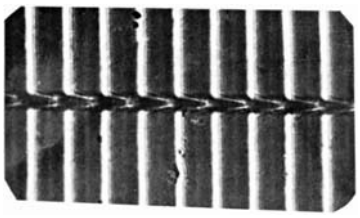

Plate (3-f)

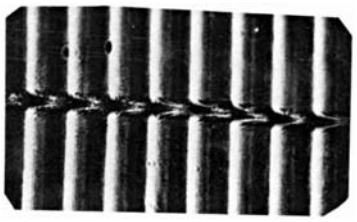

Plate (3-c)

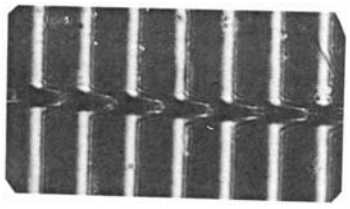

Plate (3-g)

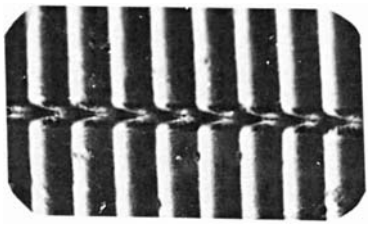

Plate (3-d)

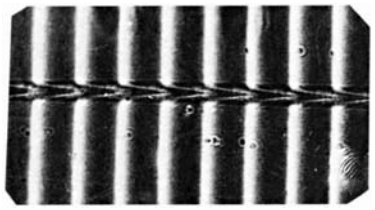

Plate (3-h)

Plate 3 (a-h)

Plate 3 (a–h) Microinterferograms of multiple-beam Fizeau fringes in transmission for the perpendicular directions of PET fiber with annealing temperatures of 80–190°C, respectively, at a constant time of 5 h.

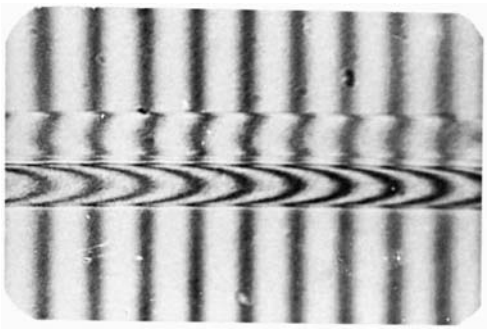

Plate (4-a)

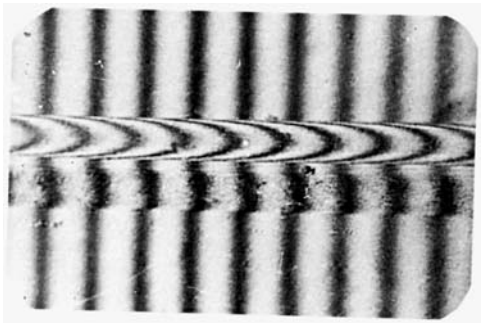

Plate (4-b)

Plate 4 (a,b) Two-beam interferograms of a totally duplicated image for the parallel and perpendicular directions of untreated PET fibers.

ometric methods are extremely sharp and the amount of information in this case is considerable.

For the determination of the refractive index of the fiber having layers of circular cross sections, El-Nicklawy and Fouda[21] derived an expression for the size of the fringe shift $dZ^{\parallel}$ at any point x along the diameter of a multiskin fiber. In a case having only a skin–core fiber, their expression leads to the following formula:

$$(\lambda/4h)dZ = (n_s^{\parallel} - n_L)(r_s^2 - x^2)^{1/2} + (n_c^{\parallel} - n_s^{\parallel})(r_c^2 - x^2)^{1/2} \quad (4)$$

where $n_s^{\parallel}$ and $n_c^{\parallel}$ are refractive indices of the skin and core, respectively, for the plane-polarized light vibrating parallel to the fiber axis; n_L, the refractive index of the immersion liquid; r_s and r_c, the radii of skin and core layers, respectively; h, the liquid interfringe spacing; and λ, the wavelength of the monochromatic light used. An analogous formula for eq. (4) is used for plane-polarized light vibrating perpendicular to the fiber axis, for the determination of both $n_s^{\perp}$ and $n_c^{\perp}$.

The mean refractive index $n_a^{\parallel}$ of polyester fibers, having a core of thickness t_c and refractive index $n_c^{\parallel}$, surrounded by a skin layer of thickness t_s and refractive index $n_s^{\parallel}$, is calculated using the formula[22]

$$n_a^{\parallel} = n_c^{\parallel}(t_c/t_f) + n_s^{\parallel}(t_s/t_f) \quad (5)$$

where t_f is the whole fiber thickness.

Two-Beam Technique

For the determination of the mean refractive indices and birefringence, the Pluta polarizing interference microscope was used.[23,24] The following equations are used to determine these optical properties[25]:

$$n_a^{\parallel} = n_L + F^{\parallel}\lambda/(Ah)$$

$$n_a^{\perp} = n_L + F^{\perp}\lambda/(Ah) \quad (6a)$$

$$\Delta n_a = \Delta F\lambda/(Ah) \quad (6b)$$

where $n_a^{\parallel}$ and $n_a^{\perp}$ are, respectively, the refractive indices of the fiber for light vibrating parallel and perpendicular to the fiber axis; n_L, the refractive index of the immersion liquid; $F^{\parallel}$ and $F^{\perp}$, the area enclosed under the fringe shift as it crosses the fiber; h, the interference fringe spacing corresponding to the wavelength λ; and A, the mean cross-sectional area of the fiber. Also, Δn_a is the birefringence of the fiber, and ΔF, the area enclosed under the fringe shift using the nonduplicated image of the fiber.

RESULTS AND DISCUSSION

Plate 1 (a) and (b) show microinterferograms of the multiple-beam Fizeau fringes in transmission of untreated PET fiber. Monochromatic light of wavelength 546.1 nm vibrating parallel and perpendicular to the fiber axis was used. The refractive indices of the immersion liquid were 1.601 and 1.5695 for the two directions of interferograms at 31°C, respectively.

The fringe shifts in the fiber were found to be toward the apex of the interferometer for the inter-

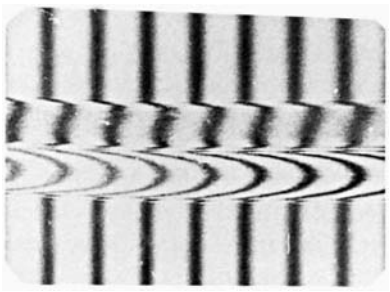

Plate (5-a)

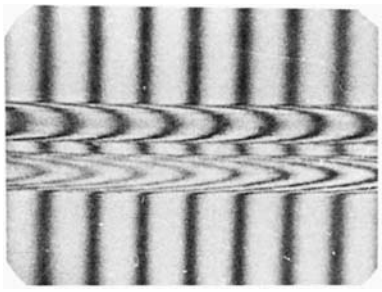

Plate (5-c)

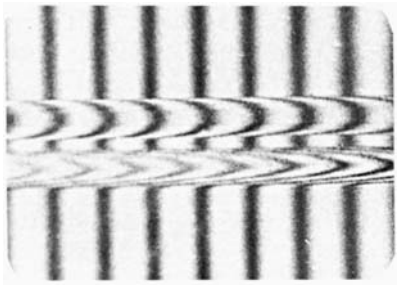

Plate (5-b)

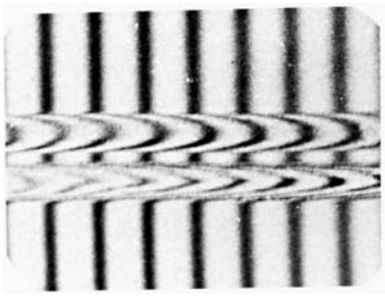

Plate (5-d)

Plate 5 (a–d) Two-beam interferograms of a totally duplicated image for the parallel directions of PET fibers with annealing temperatures of 80–190°C, respectively, at a constant time of 5 h.

ferograms 1(a) and (b). This means that the refractive indices of the chosen liquids is smaller than those of the fibers.

Plate 2(a)–(d) show interferograms of the multiple-beam Fizeau fringes in transmission of PET fiber with annealing temperatures of 80, 100, 120, and 140°C, respectively, at a constant time of 5 h.

There are remarkable limits to the use of the immersion liquid to determine the parallel direction with the application of multiple-beam Fizeau fringes in transmission. These limitations are due to the need for a higher refractive index liquid which could be suitable to observe the shift beginning and that would not react with the fiber and the coating of the optical flats, which is not now available. So, our measurements stopped at 140°C only for the parallel direction. The refractive index of the immersion liquid was 1.601 for the interferograms 2(a), and for interferograms 2(b), equal to 1.616, while for the 2(c) and (d), $n_L = 1.656$ at 20°C. The value of the fringe shift, dZ, and the interfringe spacing h and the thicknesses of the fiber, core, and skin, t_f, t_c, and t_s, were measured, respectively, on the interferograms. From eqs. (4) and (5), the skin, core, and mean refractive indices of PET fibers can be calculated.

Plate 3(a)–(h) shows interferograms of multiple-beam Fizeau fringes in transmission for the

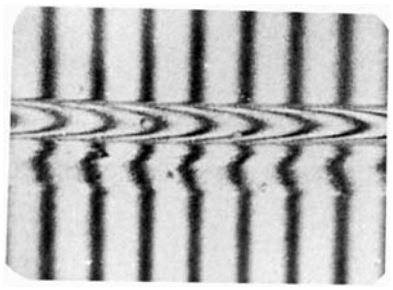

Plate (6-a)

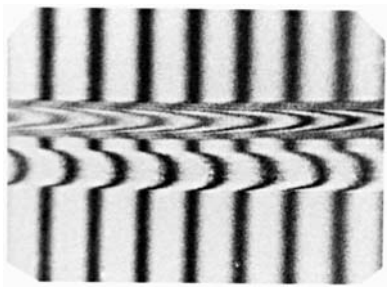

Plate (6-c)

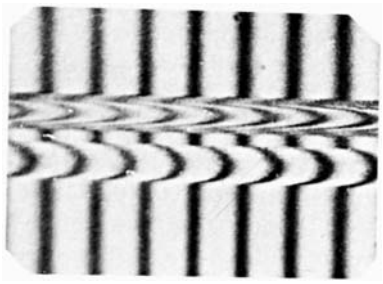

Plate (6-b)

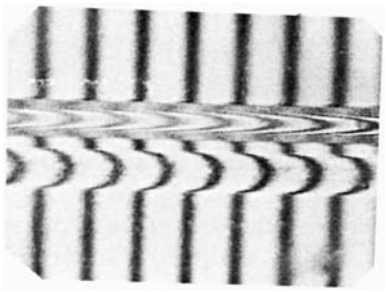

Plate (6-d)

Plate 6 (a–d) Two-beam interferograms of a totally duplicated image for the perpendicular directions of PET fibers with annealing temperatures of 80–190°C, respectively, at a constant time of 5 h.

perpendicular directions of PET fiber with annealing temperatures of 80, 100, 120, 140, 160, 170, 180, and 190°C, respectively, at a constant time of 5 h. The refractive index of the immersion liquid was 1.5695 for the interferograms at 31°C. The fringe shifts in the fiber were found to be toward the apex of interferometer for the interferograms 3(a) and (b). This means that the refractive indices of the chosen liquids is smaller than those of the fibers.

Plate 4(a) and (b) are two-beam interferograms of a totally duplicated image of untreated polyester fibers. A monochromatic light of wavelength 546.1 nm vibrating parallel and perpendicular to the fiber axis was used. The refractive indexes of the immersion liquid were 1.665 and 1.5695 for the interferograms at 18°C, respectively.

Plate 5(a) and (d) shows two-beam interferograms of a totally duplicated image of polyester fibers with different annealing temperatures at a constant annealing time of 5 h in the parallel direction. The refractive index of the immersion liquid was 1.656 at 18°C.

Plate 6(a) and (d) shows two-beam interferograms of a totally duplicated image of polyester fibers with different annealing temperatures at a constant annealing time of 5 h in the perpendicular direction. The refractive index of the immersion liquid was

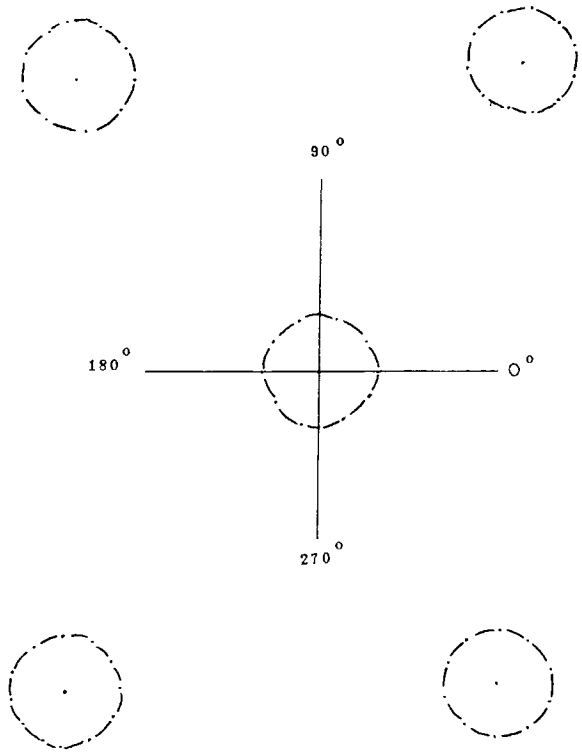

Figure 1 Experimental results for the cross-sectional view of PET fibers.

1.569 at 18°C. A monochromatic light of wavelength 546.1 nm was used.

The mean refractive indices $n_a^{\parallel}$, $n_a^{\perp}$, and Δn_a were determined using eq. (6a) and (6b). Figure 2 gives the relationship between the mean refractive indices $n_a^{\parallel}$ and $n_a^{\perp}$ with different temperatures (80–190°C) at a constant time of 5 h for polyester fiber using a

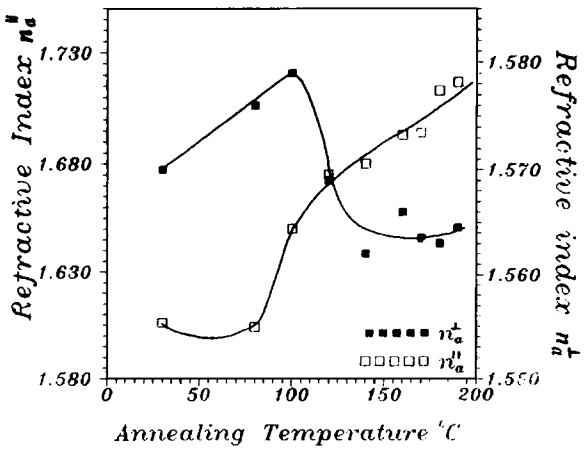

Figure 2 Relationship between the mean refractive indices $n_a^{\parallel}$ and $n_a^{\perp}$ with different temperatures of 80–190°C at a constant time of 5 h for PET fiber.

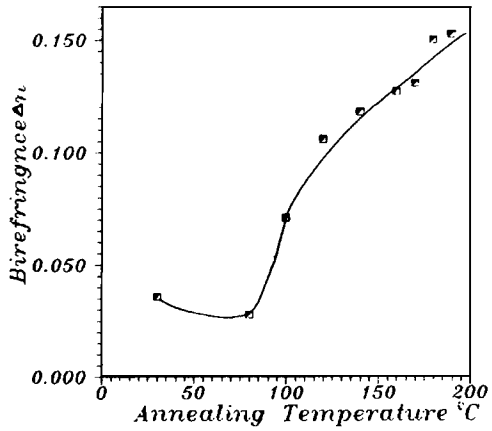

Figure 3 Relationship between the mean birefringence Δn_a with different temperatures of 80–190°C at a constant time of 5 h for PET fiber.

monochromatic light of wavelength 546.1 nm. The variation of $n_a^{\parallel}$ and $n_a^{\perp}$ of annealed polyester fibers by increasing the annealing temperature (annealing time 5 h) was obtained using a Pluta double-beam interference microscope. It is clear that the temperature of annealing increased followed by a slight decrease in $n_a^{\parallel}$ until 80°C and then it increased up to 190°C for $n_a^{\parallel}$. Also, the variation of $n_a^{\perp}$ of annealed polyester fibers by increasing the annealing temperature clarify that $n_a^{\perp}$ increases with increased annealing temperature to 100°C and then decreases to 190°C. From Figure 2, we observe that the behavior of $n_a^{\parallel}$ and $n_a^{\perp}$ was attributed to disorientation of the mobility of molecules in the parallel and perpendicular directions. Also, this behavior is proof

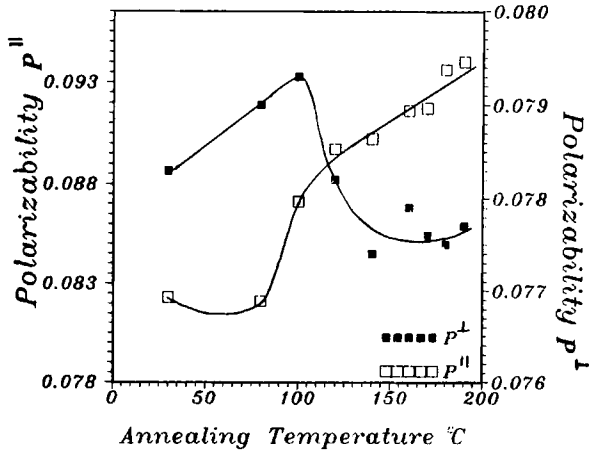

Figure 4 Relation between the mean polarizability per unit volume $P^{\parallel}$ and $P^{\perp}$ with different temperatures at a constant time 5 h for PET fibers in parallel and perpendicular directions.

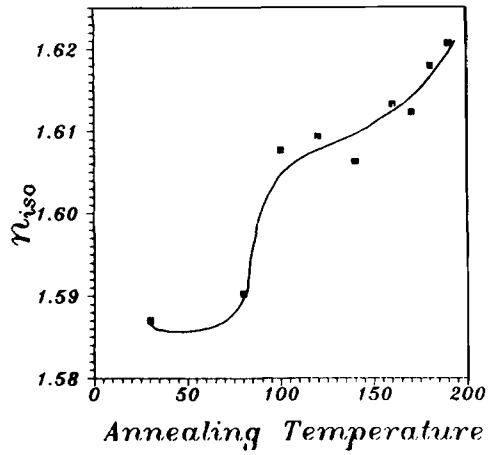

Figure 5 Relationship between n_{iso} with different annealing temperatures at a constant time of 5 h for PET fibers.

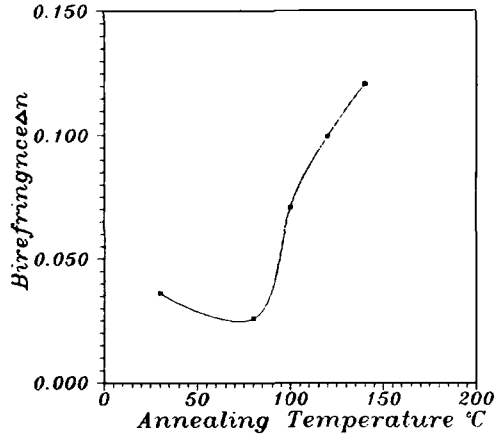

Figure 7 Relationship between the mean birefringence Δn_a and annealing temperature at a constant time (5 h) for PET fibers.

that the structure of the fiber along its axis is different from that across its axis.

Figure 3 gives the relationship between the mean birefringence Δn_a and the different temperatures (80–190°C) at a constant time of 5 h for polyester fibers using a monochromatic light of wavelength 546.1 nm.

The resultant data of the refractive indices for plane-polarized light vibrating parallel and perpendicular to the fiber axis are used in the calculation of the mean polarizability per unit volume according to the Lorantz–Loranz equation:

$$P^{\parallel} = 3/4\Pi\{[n_a^{\parallel} - 1]/[n_a^{\parallel} + 2]\} \qquad (7)$$

and a similar equation for the perpendicular direction.

Figure 4 gives the relation between the mean polarizability per unit volume $P^{\parallel}$ and $P^{\perp}$ with different temperatures at a constant time 5 h for PET fibers in parallel and perpendicular directions, which is similar to $n_a^{\parallel}$ and $n_a^{\perp}$ in Figure 2.

Just as birefringence yields information about the crystallinity and orientation of the polymer molecular chains, the isotropic refractive index of a medium also gives information not only about the molecular backage but also specifications of the unit cell of crystalline part of the medium. Hannes[26] used the following formula:

$$n_{iso} = (n_a^{\parallel} + 2n_a^{\perp})/3$$

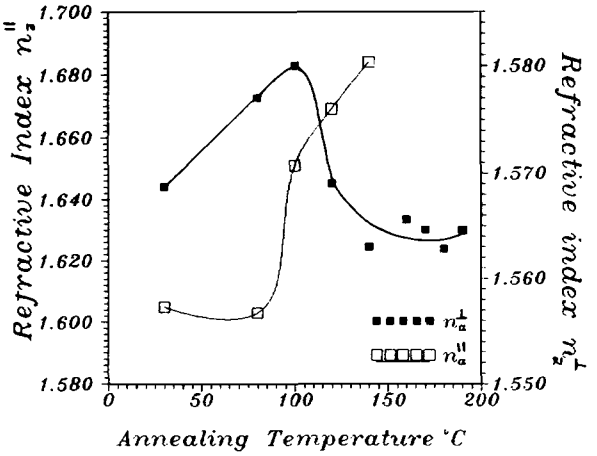

Figure 6 Relationship between the mean refractive index $n_a^{\parallel}$ and $n_a^{\perp}$ with annealing temperature at a constant annealed time (5 h) for PET fibers using multiple-beam Fizeau fringes in transmission.

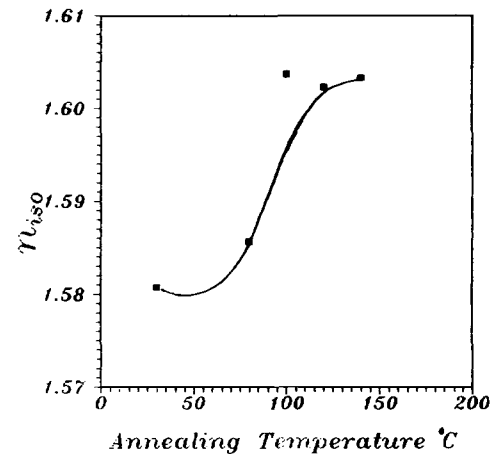

Figure 8 Relationship between the mean isotropic refractive index n_{iso} and annealing temperature at a constant annealing time (5 h) for PET fibers.

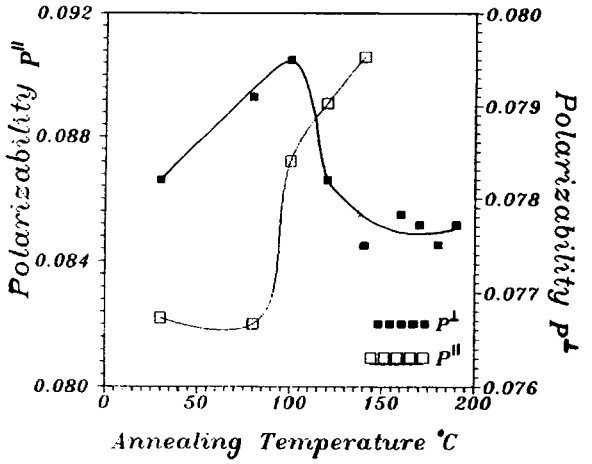

Figure 9 Relationship between the mean polarizability per unit volume $P^{\parallel}$ and $P^{\perp}$ with different temperatures at a constant time (5 h) for PET fibers in parallel and perpendicular directions.

to estimate a relation showing the crystallization in homogeneity for some types of polymers. The obtained values of $n_a^{\parallel}$ and $n_a^{\perp}$ from the interferometric techniques are used to determine the isotropic refractive index values for annealed polyester fibers.

Figure 5 shows the variation of n_{iso} of (PET) polyester fibers due to the changing of the annealing temperature at a constant time of 5 h. Figure 5 shows that the n_{iso} of PET is increased with different rates, which gives information about the molecular backage for different ranges of temperatures. From our data, we determined the constant K for different annealing temperatures at constant time of 5 h using the well-known Gladestone Dala equation:

$$[(n_{iso} - 1)/\rho = K]$$

The results are shown in Table I, which indicate that the constant K varies with different annealing conditions.

Figure 6 gives the relation between the mean refractive index $n_a^{\parallel}$ and $n_a^{\perp}$ with annealing temperature at a constant annealed time (5 h) for PET fibers using the multiple-beam Fizeau fringes in transmission. Figures 7 and 8 give the relation between the mean birefringence Δn_a and the mean isotropic refractive index n_{iso} with annealing temperature at a constant time (5 h) for PET fibers.

Figure 9 gives the relation between the mean polarizability per unit volume $P^{\parallel}$ and $P^{\perp}$ with different temperatures at a constant time (5 h) for PET fibers in parallel and perpendicular directions, which are similar to $n_a^{\parallel}$ and $n_a^{\perp}$ in Figure 6. Figures 6–9 show the variation of $n_a^{\parallel}$, $n_a^{\perp}$, Δn_a, n_{iso}, $P^{\parallel}$, and $P^{\perp}$ of annealed PET fibers by increasing the annealing temperature (annealing time 5 h) as obtained by using the multiple-beam Fizeau fringes in transmission, which show behavior similar to Figures 2–5 which were obtained by the two-beam interference technique. From Figures 6–9 we observe the same conclusions which were obtained from Figures 2–5. Also, in addition, multiple-beam Fizeau fringes prove that the arrangement of the linear molecules of which it is composed are different for the parallel and perpendicular directions for the skin and core structure of the annealed samples. Table II(a) and (b) gives the calculated values of $n_s^{\parallel}$, $n_s^{\perp}$, $n_c^{\parallel}$, $n_c^{\perp}$, $P^{\parallel}$, $P^{\perp}$, and n_{iso}.

Figure 10 shows the relation between the annealed temperature (80–190°C) and the variation of the density at a constant time (5 h). From this figure, we observe that due to increasing the time of annealing to 5 h a peak appeared at 120°C and a second peak at 170°C, which means that there are two relaxations at these temperatures. Figure 11 shows the relation between the annealed temperature and the mechanical loss factor for the polyester fiber at 5 h. It thus follows from an analysis of the experimental data presented in Figure 11 that due to increasing the time of annealing to 5 h the first peak disappeared. This could be explained as due to elimination of stresses or defects between the chains of the fibrous material. So, it is proved that the macromolecular structure of polyester fibers is strongly affected by the isothermal annealing treatment.

CONCLUSION

1. The present work demonstrates and realizes

Table I Calculated Values of Constant K at Constant Annealing Time (5 h) with Different Annealing Temperatures

Annealing Temperature (°C)	n_{iso}	$n_{iso} - 1$	ρ	K
0	1.582	0.582	1.378	0.4224
80	1.585	0.585	1.685	0.3474
100	1.603	0.603	1.731	0.3482
120	1.604	0.604	1.771	0.3412
140	1.601	0.601	1.690	0.3558
160	1.608	0.608	1.555	0.3912
170	1.607	0.607	1.792	0.3389
180	1.613	0.613	1.587	0.3863
190	1.616	0.616	1.537	0.4005

Table II Refractive Indices $n_s^{\parallel}$, $n_s^{\perp}$, $n_c^{\parallel}$, and $n_c^{\perp}$ and Mean Polarizability $P^{\parallel}$, $P^{\perp}$, and n_{iso} of Annealed PET Fibers at Different Temperatures with a Constant Time of 5 H

		Annealing Temperature (°C)							
	Unannealed	80	100	120	140	160	170	180	190
(a) Refractive indices[a]									
$n_s^{\parallel}$	1.6010	1.5944	1.6673	1.6825	1.6757	—	—	—	—
$n_s^{\perp}$	1.5755	1.5755	1.5755	1.5755	1.5755	1.5755	1.5755	1.5755	1.5755
$n_c^{\parallel}$	1.6076	1.6072	1.6436	1.6821	1.6893	—	—	—	—
$n_c^{\perp}$	1.5651	1.5653	1.5777	1.5664	1.5569	1.5606	1.5591	1.5572	1.5591
(b) Mean polarizability[b]									
$P^{\parallel}$	0.0822	0.082	0.0872	0.0891	0.0906	—	—	—	—
$P^{\perp}$	0.0782	0.0791	0.0795	0.0782	0.0775	0.0778	0.0777	0.0775	0.0777
n_{iso}	1.5808	1.5857	1.6037	1.6023	1.6033	—	—	—	—

[a] λ = 546.1 nm. Multiple-beam interference technique. Values have accuracy of 7×10^{-4}.
[b] Multiple-beam Fizeau fringes were used. λ = 546.1 nm.

the applicability of a vibrating system technique to determine the density and the mechanical loss factor (tan δ) with good accuracy to detect small variations. This resonance technique is quick, nondestructive, and accurate (expected error is below 1%).

2. Interferometric studies made it possible to determine the principal refractive indices of the fiber and its birefringence, which are valuable parameters in correlation of the structural properties of the fiber with its thermal properties.
3. The direction dependence of the refractive indices having unequal behavior in different directions was demonstrated. Clearly, this behavior is proof that the structure of the fiber along its axis is different from that across its axis. The arrangement of the linear molecules of which it is composed are different in the parallel direction from that in the perpendicular one (see Figs. 2 and 6).
4. The loss tangent (tan δ) greatly depends on the thermal energy of the intermolecular interaction, which affects the molecular motion in PET fibers. Also, tan δ is indicative of the effect of a structural transformation change on the thermal properties of polyester fibers.
5. The change of isotropic refractive indices is

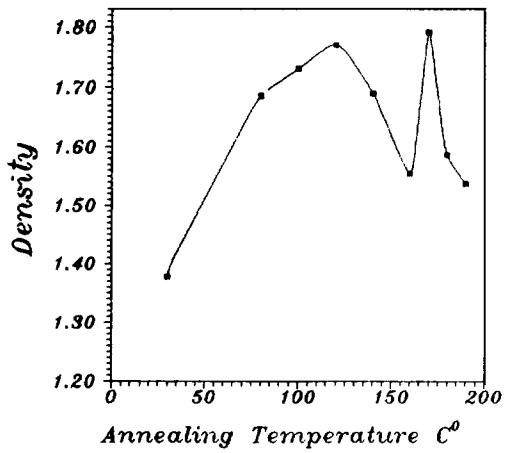

Figure 10 Relationship between the density, ρ, with different annealing temperatures at a constant time (5 h) for PET fibers.

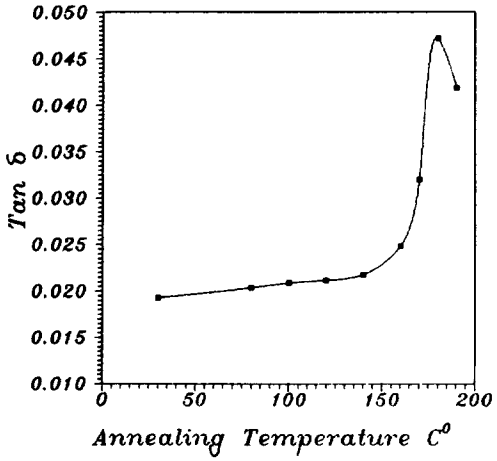

Figure 11 Relationship between the mechanical loss factor, tan δ, with different annealing temperatures at a constant time (5 h) for PET fibers.

related to the degree of order and crystallinity of the fiber as well as to the density of sample.

6. The produced microinterferograms clarify the difference in optical path variations due to annealed and unannealed fibers.
7. The results shown in Table I indicate that the constant K varies with different annealing conditions.

From the above results and considerations, we concluded that the practical importance of these measurements provides acceptable results for the optothermal and mechanical parameters.

REFERENCES

1. A. E. Zachariades and R. S. Porter, in *The Strength and Stiffness of Polymers,* Marcel Dekker, New York, 1983, pp. 20–21.
2. H. deVries, *J. Polym. Sci.,* **34,** 761 (1959).
3. I. M. Fouda and M. M. El-Tonsy, *J. Mater. Sci.,* **25,** 121 (1990).
4. I. M. Fouda, M. M. El-Tonsy, and A. H. Oraby, *J. Mater. Sci.,* **25,** 1416 (1990).
5. A. A. Hamza, I. M. Fouda, M. A. Kabeel, and H. M. Shabana, *Polym. Test.,* **8,** 201 (1989).
6. A. A. Hamza, I. M. Fouda, K. A. El-Farhaty, and E. A. Seisa, *Polym. Test.,* **10,** 83 (1991).
7. I. M. Fouda and M. M. El-Tonsy, *J. Mater. Sci.,* **25,** 4752 (1990).
8. I. M. Fouda, M. M. El-Tonsy, and H. M. Hosny, *Polym. Degrad. Stabil.,* **46,** 287 (1994).
9. W. H. Wyckoff, *J. Polym. Sci.,* **68,** 83 (1962).
10. W. O. Statton, *J. Polym. Sci. Part A2,* **10,** 1987 (1972).
11. S. N. Maurthy, H. Minor, and A. J. Latis, *Macromol. Sci. Phys. B,* **26**(4), 427 (1987).
12. D. Hofmann, R. Leonhardt, and P. J. Weigel, *Appl. Polym. Sci.,* **46,** 1025 (1992).
13. A. A. Hamza, I. M. Fouda, T. Z. N. Sokker, M. M. Shahin, and E. A. Seisa, *J. Mater. Sci.,* to appear.
14. I. I. Perepechko, *An Introduction to Polymer Physics,* Mir, Moscow (English translation, 1981), Chap. 7, p. 216.
15. S. M. Curry and A. L. Schawlow, *Am. J. Phys.,* **42,** 12 (1974).
16. I. M. Fouda, M. M. El-Tonsy, and A. M. Shaban, *J. Mater. Sci.,* **26,** 5085 (1991).
17. A. A. Hamza, I. M. Fouda, M. M. El-Tonsy, and F. M. El-Sharkawy, *J. Appl. Pol. Sci.,* **56,** 1355 (1995).
18. N. Subrahmanyam and B. Lal, *A Text Book of Sound,* 2nd ed., Vikas, New Delhi, 1979, p. 143.
19. E. Schreiber, O. L. Anderson, and N. N. Soga, *Elastic Constants and Their Measurement,* McGraw-Hill, New York, 1973, p. 367.
20. V. T. Cherepin and A. K. Mallik, *Experimental Techniques in Physical Metallurgy,* Indian Institute of Technology, Bombay Series, Asia Publishing, 1967, p. 82.
21. M. M. El-Nicklawy and I. M. Fouda, *J. Text. Inst.,* **71,** 257 (1980).
22. N. Barakat and H. A. El-Hennawi, *Text. Res. J.,* **41,** 391 (1971).
23. M. Pluta, *Opt. Acta,* **18,** 661 (1971).
24. M. Pluta, *J. Microsc.,* **96,** 309 (1972).
25. A. A. Hamza, T. Z. N. Sokker, and M. A. Kabeel, *J. Phys. D Appl. Phys.,* **18,** 1773 (1985).
26. H. Hannes, *Z. Z. Kolloid Polym.,* **250,** 765 (1972).

Received June 8, 1995
Accepted September 18, 1995